Journal of Advanced Research in Numerical Heat Transfer

Journal homepage:
https://semarakilmu.com.my/journals/index.php/arnht/index
ISSN: 2735-0142

Application of the Phase Field Approach for Crack Propagation in Viscoelastic Solid Materials under Thermal Stress: A Case Study of Solder Fracturing

Sayahdin Alfat[1,*], La Ode Ahmad Barata[2], Aditya Rachman[2], Rosliana Eso[1], Arman[3], Nurgiantoro[4], Ali Mulya Rende[5]

[1] Physics Education Department, Faculty of Teacher Training and Education, Halu Oleo University, H.E.A. Mokodompit, Kendari, 9323, Southeast Sulawesi, Indonesia
[2] Mechanical Department, Faculty of Engineering, Halu Oleo University, H.E.A. Mokodompit, Kendari, 9323, Southeast Sulawesi, Indonesia
[3] Mathematics Department, Faculty of Mathematics and Natural Sciences, Halu Oleo University, H.E.A. Mokodompit, Kendari, 9323, Southeast Sulawesi, Indonesia
[4] Geography Department, Faculty of Mathematics and Natural Sciences, Halu Oleo University, H.E.A. Mokodompit, Kendari, 9323, Southeast Sulawesi, Indonesia
[5] Department of Elementary School Teacher Education, Halu Oleo University, H.E.A. Mokodompit, Kendari, 9323, Southeast Sulawesi, Indonesia

ARTICLE INFO

Article history:
Received 20 September 2024
Received in revised form 22 October 2024
Accepted 19 November 2024
Available online 15 December 2024

Keywords:
Phase field model; Thermal fracturing; Viscoelasticity; Solder cracking; Adaptive mesh refinement

ABSTRACT

To date, solder has been a crucial component for interconnecting circuit boards (PCBs) and electronic components in the electronics industry. However, solder faces certain challenges, such as cracking due to thermal changes. This paper investigates solder cracking under thermal expansion. We employ a phase field model to study crack propagation under thermal stress in a square domain and in solder with a fillet shape. The model is based on those proposed by Takaishi-Kimura and Alfat, where the stress and strain tensors are modified to account for variations in the temperature field. In this study, we consider the solder material to be viscoelastic, while the other materials are treated as homogeneous and isotropic. A numerical example is computed using the adaptive mesh finite element method, with the code implemented in FreeFEM software. The results of this study are in good agreement with previous numerical and experimental findings.

1. Introduction

There are many factors that can enhance crack propagation, and changing tem perature is one of them [1]. Since thermal effects within an elastic body are accompanied by shifts in the relative positions of the particles composing the body [2], this phenomenon is called thermoelasticity. In the electronics industry, this phenomenon can cause solder cracking. Experimentally, there are three methods to observe and predict the mechanism of solder cracking: (a) the high-temperature storage test [2], (b) the temperature cycle test or air chamber method [3,4], and (c) the thermal shock test

* *Corresponding author.*
E-mail address: sayahdin.alfat@yahoo.com (Sayahdin Alfat)

https://doi.org/10.37934/arnht.28.1.94108

[3,4]. However, laboratory experiments often encounter several obstacles. For instance, since the solder size is small, the experimental collection of stress-strain data is becoming increasingly difficult [5]. Therefore, one simple alternative to tackle it is numerical simulation [6].

The discrete model is a fundamental element of numerical methods, extensively used to tackle real-world engineering problems. Among these models, the extended finite element method (XFEM) is particularly notable for its effectiveness in structural and continuum mechanics. However, XFEM faces difficulties when dealing with complex geometries and three-dimensional extensions without adding new vertices. Furthermore, the integration of the gradient is complicated by singularities and discontinuities [7]. Consequently, an alternative model is necessary. One promising alternative is the phase field model (PFM). The PFM is both a fascinating mathematical concept and a robust method [8-11]. The phase field model (PFM) is one kinds of continuous approach which is powerful model. It has been employed in various simulations, including crack propagation [12-14], solidification [15-17], crystal growth [18-19], multicellular systems [20,21], incompressible fluids [22,23], and dislocation [24]. This approach has become well-established for modeling the development of non-equilibrium microstructures.

Essentially, several studies on solder cracks using phase field model (PFM) have been conducted effectively [8,25]. Among them, the research reported by Kimura and colleagues [8] presents a simple model that effectively explains solder cracking due to temperature changes. Although this model has successfully elucidated the behavior of crack growth in solder resulting from thermal variations, we believe it can be modified by adjusting the crack's driving force and considering the solder as a viscoelastic solid. Therefore, building upon the studies from [26-28], we propose an alternative model to describe solder crack behavior under temperature changes by considering the solder material as a viscoelastic solid. From a simulation point-of-view, we apply the Kelvin-Voigt type viscoelasticity model in the present study due to its simplicity.

Considering solder as a viscoelastic solid is reasonable, as its mechanical properties exhibit a combined response of elastic and viscous behavior when subjected to varying loads or temperature changes [29-31]. Among the various types of viscoelastic models, one of the simplest is the Kelvin-Voigt model, which describes the immediate viscoelastic response of solder material under stress [32]. Although the Kelvin-Voigt model offers simplicity, it does not fully capture long-term creep or stress relaxation. However, these limitations become less significant when the study focuses solely on the initial stages of crack propagation and small deformation conditions [33,34]. Therefore, the Kelvin-Voigt viscoelastic model is a reasonable choice for describing and investigating crack behavior in solder material, even without the inclusion of other viscoelastic models, which are more complex.

The aim of this paper is to develop a numerical method for simulating solder fracturing under thermal stress, considering solder as a viscoelastic material. A primary focus of this research is to investigate the behavior of crack propagation under cyclic thermal stress. In the simulation, the computational domain assumes that only the solder is a viscoelastic solid, while other materials, such as printed circuit boards (PCBs), semiconductor components, and Cu patterns, are considered rigid bodies. We believe that our current research using the phase field model has not been conducted by other researchers. While similar studies have been done, they consider only solder material with linear elasticity [8,25,35].

This paper is structured into five main sections. In Section 2, we examine the governing equation of crack propagation resulting from thermal expansion. This section also presents a computational model, including boundary and initial conditions, as well as all relevant physical properties. Additionally, the solder joint geometry, including the shape and size of the solder, is shown in this section. In the present study, we did not investigate the effect of solder joint geometry on crack propagation behavior and have only selected the fillet shape. However, readers can refer to [8] for

more on the impact of solder joint geometry on crack propagation behavior. Section 3 describes the numerical method and algorithm used to simulate crack behavior under thermal stress. Since we apply the refinement mesh technique, this section also addresses the adaptive finite element method. In Section 4, we present the numerical results of solder cracking and discuss them alongside a physical analysis. Finally, Section 5 concludes with the main findings and suggests possible future research directions as extensions of this study.

2. Mathematical Model and Computational Model

2.1 Governing Equation

In the present paper, we study crack propagation under thermal stress in eutectic solder material cases. Herein, the study develops the phase field model for thermal cracking by modifying the thermal fracturing model in [8] with the temperature function given and the thermal fracturing for viscoelastic solids in [27]. Therefore, the phase field model for thermal fracturing is given by

$$\begin{cases} -\mathrm{div}\left((1-z)^2\left(\sigma_{\mathrm{kv}}\left[u, e[\dot{u}]\right] - \beta(\Theta-\Theta_0)I\right)\right) = f(x,t) & x \in \Omega, \\ \alpha\dfrac{\partial z}{\partial t} = \left(\epsilon\mathrm{div}(\gamma(\mathrm{x})\nabla\mathrm{z}) - \dfrac{\gamma(\mathrm{x})}{\epsilon}z + (1-z)\mathrm{W}(\mathrm{u})\right)_+ & x \in \Omega, \end{cases} \tag{1}$$

where Ω is a bounded two-dimensional domain $\Omega \subset R^2$, $\gamma(x)$ is the critical energy release rate $[\mathrm{Pa}\cdot\mathrm{m}]$ with respect to position, $f(x,t)$ is the external force $[\mathrm{Pa}\cdot\mathrm{m}^{-1}]$, $u(x,t)$ represents the displacement vector $[\mathrm{m}]$ at position $x = (x_1, x_2)^T \in \Omega$ and time $t \geq 0$ $[\mathrm{s}]$, and the function $z(x,t)$ is called the phase field for crack shape. The variable $z(x,t)$ satisfies $0 \leq z(x,t) \leq 1 \in \Omega$, where $z = 0$ represents the uncracked area and $z = 1$ represents the cracked area. The parameters $\alpha > 0$ and $\epsilon > 0$ represent, respectively, small numbers related to regularization in time $[\mathrm{Pa}\cdot\mathrm{s}]$ and space $[\mathrm{m}]$. Some researchers refer to ϵ as the length scale parameter [9,13]. The parameters Θ and Θ_0 are the given temperature $[\mathrm{K}]$ and initial temperature $[\mathrm{K}]$, respectively. In addition, the thermal modulus is defined by $\beta = a_L(\mathrm{d}\lambda + 2\mu)$ $[\mathrm{Pa}\cdot\mathrm{K}^{-1}]$, where $a_L > 0$ is called the coefficient of linear thermal expansion $[\mathrm{K}^{-1}]$. The strain and stress tensors for Kelvin-Voigt type viscoelastic solids are respectively defined by:

$$e_{kv}\left[u, e[\dot{u}]\right] = e[u] = e_{ij}[u], \qquad e_{ij}[u](x) \coloneqq \frac{1}{2}\left(\frac{\partial u_i}{\partial x_j}(x) + \frac{\partial u_j}{\partial x_i}(x)\right) \quad (i,j = 1,2), \tag{2}$$

$$\sigma_{kv}\left[u, e[\dot{u}]\right] \coloneqq C_1 e[u] + \mathrm{C}_2 e[\dot{u}], \tag{3}$$

where C_1 and C_2 are the elastic tensor [Pa] and viscosity constant $[\mathrm{Pa}\cdot\mathrm{s}]$, respectively, while $e[\dot{u}]$ is the partial derivative of the strain tensor with respect to t. $\sigma[u] = C_1 e[u]$ is called the stress tensor, which is defined as follows:

$$\sigma[u] \coloneqq \lambda(\mathrm{div}u)I + 2\mu e[u],$$

where $\mathrm{div}u \coloneqq \mathrm{tr}(e[u]) = \left(\dfrac{\partial u_1}{\partial x_1} + \dfrac{\partial u_2}{\partial x_2}\right)$ is the volumetric strain tensor and I is the identity matrix.

In the second row of Eq. (1), $W(u)$ is called the elastic energy density, which represents the driving force of crack propagation. It is defined by the following equalities:

$$\begin{aligned} \mathrm{W(u)} &:= \sigma[u]: e[u] = (\lambda(\mathrm{div}u)I + 2\mu e[u]): e[u] \\ &= \lambda(\mathrm{div}u)^2 + 2\mu|e[u]|^2 \end{aligned} \tag{4}$$

The parameters $\lambda = \frac{E_Y \nu_P}{(1+\nu_P)(1-2\nu_P)}$ and $\mu = \frac{E_Y}{2(1-\nu_P)}$ are Lame's constants $[\mathrm{Pa}]$, where the constants $E_Y > 0$ and $\nu_P > 0$ represent Young's modulus $[\mathrm{Pa}]$ and Poisson's ratio $[-]$, respectively. There are two notes related to the driving force of crack propagation. First, we have chosen the thermoelastic energy density $W(u,\Theta) = \sigma[u,\Theta]: e[u,\Theta]$ as the driving force for crack propagation in a previous study [8]. Second, Eq. (4) can be split into $\lambda^*(\mathrm{div}\, u)_+^2 + 2\mu|e_D[u]|^2$ dan $\lambda^*(\mathrm{div}\, u)_-^2$, which represent the positive and negative parts of the elastic energy density, respectively. We can then consider the positive part of the elastic energy density as the driving force of crack propagation. It should be noted that it is not necessarily applied immediately; we should also split the $(1-z)^2\sigma_{\mathrm{kv}}\big[u, e[\dot{u}]\big]$ term into positive and negative parts in Eq. (1). For details, the reader can refer to [27]. In the current study, we have not investigated this further.

If we denote the total stress tensor, including the damage variable, as $\sigma_z^*[u, e[\dot{u}], \Theta] := (1-z^2)\big(\sigma_{\mathrm{kv}}\big[u, e[\dot{u}]\big] - \beta(\Theta - \Theta_0)I\big)$, we can write the first row of Eq. (1) as $-\mathrm{div}(\sigma_z[u, e[\dot{u}], \Theta]) = f(x,t)$. Hereafter, we will omit $f(x,t)$ for simplicity. Eq. (1) is complemented by the boundary and initial conditions, as follows:

$$\begin{cases} u = u_D(x,t) & \text{on } \Gamma_D, \\ \sigma_z^*[u, e[\dot{u}], \Theta]n = q(x) & \text{on } \Gamma_N, \\ \frac{\partial z}{\partial n} = 0 & \text{on } \Gamma, \\ u(x,0) = u_0(x) & x \in \Omega, \\ z(x,0) = z_0(x) \in [0,1] & x \in \Omega, \end{cases} \tag{5}$$

where $u_0(x)$ is the initial displacement, $z_0(x)$ is the initial crack, n is the normal vector, $u_D(x,t)$ is the given displacement on the Dirichlet boundary Γ_D, and $q(x)$ is the given boundary load on the Neumann boundary Γ_N. The boundary Γ is defined $\partial\Omega := \Gamma_{\mathrm{D}} \cup \Gamma_N$.

2.2 Computational Model

This section will discuss the computational realm, computational arrangement, and fundamental constants for thermal fracturing in a 2D solder domain. Additionally, it outlines certain assumptions made regarding the physical aspects during calculations. To begin, we will elucidate the computational domain.

Models concerning solder joint fatigue or solder cracking stem from empirical stress, strain, and energy data derived from thermal cycling experiments. In numerical simulations, we designate the fillet shape as the computational domain (see Figure 1). We did not design the solder joint with a volcano shape [8] or a shape suitable for connecting a quad flat package to the PCB [36].

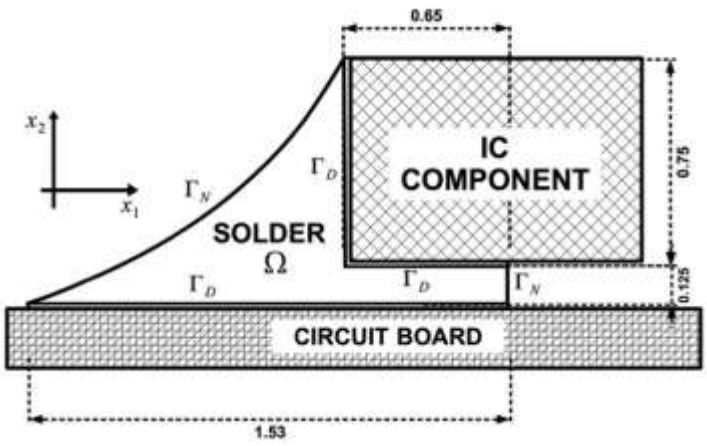

Fig. 1. Computational domain of thermoelasticity problem

In this paper, we simulate crack propagation in eutectic 36Sn-37Pb solder. Since we consider the fillet shape, the domain in Figure 1 can be divided into the Neumann boundary Γ_N and the Dirichlet boundary Γ_D, which are clearly defined by the following equation:

$$\begin{cases} u = 0 & \text{on } \Gamma_D, \\ \sigma_z^*[u, e[\dot{u}], \Theta]n = 0 & \text{on } \Gamma_N. \end{cases} \tag{6}$$

Herein, $\Gamma_N \cup \Gamma_D = \partial\Omega$ where $\partial\Omega$ denotes the boundary of the computational domain. In addition, we also set the initial conditions as follows:

$$\begin{cases} z_0(x) = 0 & \text{in } \Omega, \\ u_0 = 0 & \text{in } \Omega. \end{cases} \tag{7}$$

In the following example, we assume that the electronic components (e.g., integrated circuits (ICs), semiconductor chips, and printed circuit boards (PCBs)) are rigid bodies, while the solder material is treated as a viscoelastic solid. Additionally, for simplicity, the solder material is assumed to be homogeneous and isotropic. The physical properties of the solder material are set based on the thermal fracturing simulations in [8], except for the parameter ϵ. In the present paper, $\epsilon = 5 \times 10^{-3}$ is used for solder fracturing due to variations in the maximum triangle sizes. Furthermore, different from [8], we set the temperature function $\Theta(\mathrm{t})$ as $90\sin(10\pi t) + 35$ (see Figure 2), with a duration t of 5000 and a time step Δt given by 1×10^{-3}. Based on the function, we consider the effect of repeated thermal cycling. Although we understand that repeated thermal cycling has implications for crack propagation behavior, this study uses only a single temperature function. In the current study, we assume that all the parameters are nondimensional. The nondimensional setting is detailed in [8,28].

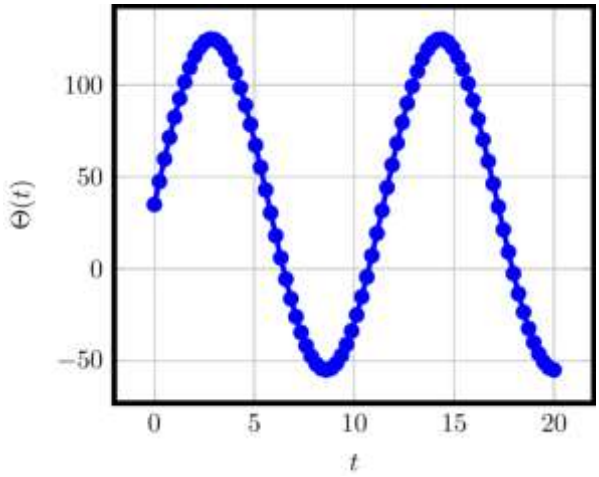

Fig. 2. Illustration of temperature function profile during the time interval $0 \leq t \leq 20$

3. Numerical Method

3.1 Finite Element Discretization and Weak Form

To simulate the solder fracturing, we solve the thermoelasticity problem in Eq. (1), we derive a semi-discretization in time t. Let u^k and z^k be the solution approximations of u and z, and we set $\Delta t > 0$ as a constant time step, with $(t_k = k\Delta t)$ $(k = 1,2,\cdots)$. The numerical solution of the thermoelasticity equation is recomputed from the solution of (u^{k-1}, z^{k-1}) with the semi-implicit scheme [12]:

$$\begin{cases} -\mathrm{div}\left((1-z^{k-1})^2\left(\sigma[u^k] + \frac{C_2}{\Delta t}(e[u^k] - e[u^{k-1}]) - \beta(\Theta - \Theta_0)I\right)\right) = 0, \\ \alpha\frac{\tilde{z}^k - z^{k-1}}{\Delta t} = \epsilon\mathrm{div}(\gamma\nabla\tilde{z}^k) - \frac{\gamma}{\epsilon}\tilde{z}^k + (1-\tilde{z}^k)\mathrm{W}(\mathrm{u}^{\mathrm{k}}), \\ z^k = \max(\tilde{z}^k, z^{k-1}). \end{cases} \tag{8}$$

Since the critical energy release rate is constant, we simplify Eq. (8) by writing $\gamma(x) = \gamma$. In the Eq. (8), the term $z^k = \max(\tilde{z}^k, z^{k-1})$ represents $(\cdot)_+$ in the Eq. (1).

Now, we derive the weak form of Eq. (8). Let $(v \in H^1(\Omega)|v = 0 \text{ on } \Gamma_D)$ be a test function for the first row in Eq. (8) and $(w \in H^1(\Omega)|w = 0 \text{ on } \Gamma)$ for the second row in Eq. (8). Then, we can write the weak form of the Eq. (8) as follows:

For the first row:

$$\begin{aligned} \int_\Omega (1-z^{k-1})^2\sigma[u]:e[v]dx + \frac{1}{\Delta t}\int_\Omega (1-z^{k-1})^2 C_2 e[u^k]:e[v]dx \\ = \frac{1}{\Delta t}\int_\Omega (1-z^{k-1})^2 C_2 e[u^{k-1}]:e[v]dx \\ + \int_\Omega (1-z^{k-1})\beta(\Theta-\Theta_0)\mathrm{div}v dx \quad (\forall \mathrm{v} \in \mathrm{V}^{\mathrm{u}}). \end{aligned} \tag{9}$$

For the second row:

$$\tau \int_{\Omega} \left(\tilde{z}^{k} - \mathrm{z}^{\mathrm{k}-1}\right) \mathrm{wdx} = -\int_{\Omega} \epsilon\gamma \nabla \mathrm{z}^{\mathrm{k}} \cdot \nabla \mathrm{wdx} - \frac{\gamma}{\epsilon} \int_{\Omega} \tilde{z}^{k}\, \mathrm{wdx} + \int_{\Omega} (1 - \tilde{z}^{k}) \mathrm{W}\left(\mathrm{u}^{\mathrm{k}}\right) \mathrm{wdx} \quad (\forall w \in V^{z}), \tag{10}$$

where $\tau = \frac{\alpha}{\Delta t}$. Finally, we have obtained the weak form of Eq. (8). We will apply it to simulate the solder cracking problem and thermal fracturing in square domain.

As a remark, in the following numerical simulation, we apply non-dimensional parameters to facilitate the calculation process. The non-dimensional setting can be found in [8], while the derivation of transformation parameters is shown in [28].

3.2 Adaptive Mesh Finite Element Technique

We solve the governing equation of crack propagation under thermal stress, represented by Eqs. (9)-(10), using FreeFEM [37] with adaptive P2-elements technique, where z is evaluated by remeshing at each time step. For adaptive refinement, we use an error indicator criterion to identify regions of the mesh that require refinement, with an error threshold set to 0.01. As a result, we obtain a newly refined mesh. Furthermore, we must also transpose u^k and z^k onto the new refined mesh to update the values of u^k and z^k at the Gauss points of the mesh. The details of the adaptive mesh algorithm are shown in Algorithm 1. This code implements the discrete equation derived from the finite element weak formulation in Section 3.1. The main reason we choose the adaptive mesh technique is its ability to drastically reduce calculation time during the numerical process [27]. We will demonstrate the robustness of this technique in reducing computation time in Section 4.2. Additionally, we use ParaView as a visualization tool.

Algorithm 1 Crack propagation due to the cyclic thermal stress based on adaptive mesh

Input: physical parameters
Input: time parameters t_{max} and Δt
Input: Minimum h_{min} and maximum h_{max} size of triangle
Input: temperature function $\Theta(t)$
Set: Initial mesh $\mathcal{T}_{\hbar}^{0}$ and initial crack $z^{0}(x)$
For $k = 1, \cdots, T/\Delta t$ do
  Set $\mathcal{T}_{\hbar}^{k} = \mathcal{T}_{\hbar}^{k-1}$
  Calculate the solution of u^k and z^k based on Eqs. (9)-(10)
  For $i = 1, \cdots, 10$ do
    Design new mesh $\mathcal{T}_{\hbar}^{i}$ based on z^k
  End for
  Set $\mathcal{T}_{\hbar}^{k+1} = \mathcal{T}_{\hbar}^{i}$
  Interpolate u^k and z^k on new mesh $\mathcal{T}_{\hbar}^{k+1}$
End for

4. Numerical Results and Discussion

Although this study primarily focuses on solder cracks caused by thermal cycling, we will also discuss the effect of temperature on square viscoelastic solids on crack growth. This serves as a basic

verification of how temperature gradients in viscoelastic solids can accelerate crack propagation. We will cover this in Section 4.1, while the explanation of solder cracks will be provided in Section 4.2.

4.1 Thermal fracturing in square viscoelastic solids

In this section, a numerical example considers a square domain $\Omega \coloneqq [-0.5,0.5] \times [-0.5,0.5] \in R^2$ with a single initial crack. The domain is subjected to uniaxial stress in the vertical direction, as clearly illustrated in Figure 3. Since the example utilizes an adaptive finite element method, we apply Algorithm 1 to solve the thermal fracturing in square viscoelastic solids. Furthermore, the parameters used are listed in Table 1.

Table 1
Non-dimensional parameters for the case in Section *4.1*

Parameters	E_Y [-]	ν_P [-]	C_2 [-]	α [-]	ϵ [-]	γ [-]	a_L [-]	Θ_0 [-]	Δt [-]	t [-]
Value	5×10^6	0.29	2×10^4	1×10^{-3}	2×10^{-2}	2.5	1×10^{-4}	0	6×10^{-4}	2500

Since the temperature varies, we set it to $\Theta = 0.0, 2.5, 5.0, 7.5$ for instance. Additionally, the square viscoelastic solid is considered a homogeneous and isotropic material.

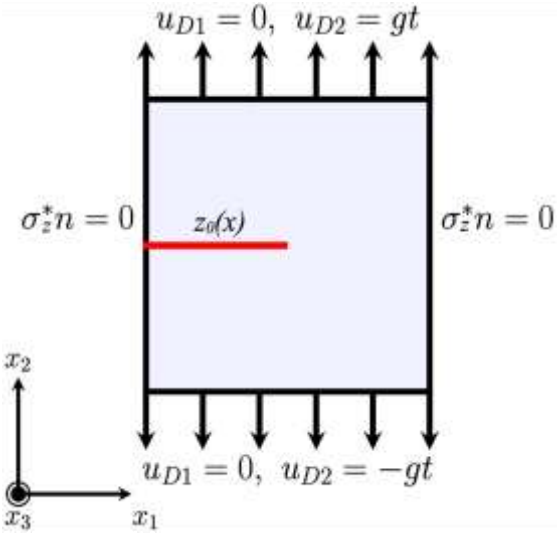

Fig. 3. Domain illustration for Section *4.1*. We set $g = 0.002$, and denote $\sigma_z^* n = \sigma_z^*[u, e[\dot{u}], \Theta]n$ for simplicity. The red line represents the initial crack

Figure 4 shows the results of thermal fracturing in square viscoelastic solid material. Since the behavior is similar, we do not show the crack propagation for temperature $\theta = 0.0$. The red color represents the cracked area, while the blue color represents the uncracked area. Because the domain is subjected to uniaxial stress in the vertical direction and is made of a homogeneous and isotropic material, the crack propagation behavior is straight, extending to the right. From Figure 4, it is evident that crack propagation is slower in the square material at higher temperatures, while it is faster in the material at lower temperatures. This behavior can be attributed to the presence of thermal stress. The higher the temperature of a material, the greater the thermal stress. This increased

thermal stress causes the total energy available for crack growth to decrease, indirectly reducing the crack propagation rate.

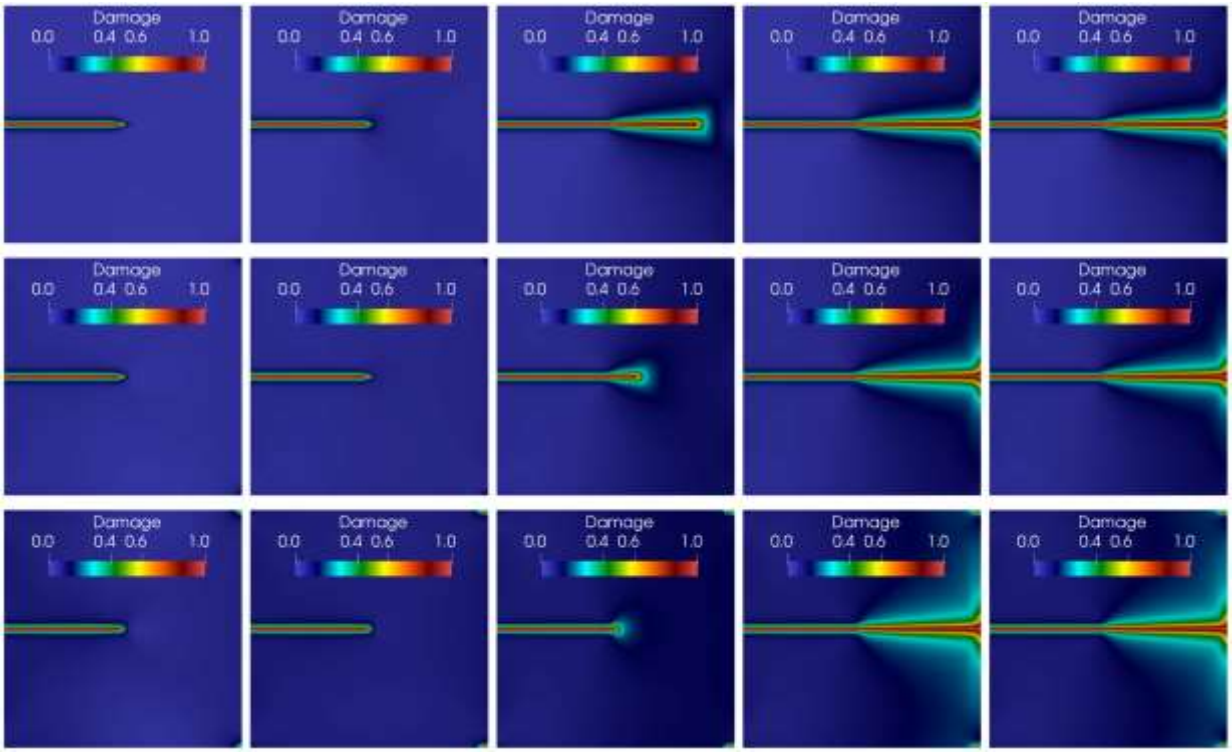

Fig. 4. Snapshot of thermal fracturing for each temperature θ variation at time $t = 0.0, 0.375, 0.75, 1.125, 1.5$ (from left to right): $\Theta = 2.5$ (top), $\Theta = 5.0$ (middle), and $\Theta = 7.5$ (bottom)

Theoretically, the speed at which a crack propagates can also be assessed using the surface energy profile. The surface energy can be determined using the following equation:

$$\mathrm{E_s(z)} = \frac{1}{2}\int_{\Omega} \gamma\left(\epsilon|\nabla z|^2 + \frac{1}{\epsilon}z^2\right)dx \tag{11}$$

The results of Eq. (11) are shown in Figure 5. It is clear that cracks propagate more slowly in high-temperature materials and more quickly in low-temperature materials. Another observation from Figure 5 is the size of the cracked area. Since crack size is proportional to surface energy, calculating the surface energy helps assess the extent of the cracked area. The Figure 5 also demonstrates that the cracked area tends to be larger in high-temperature materials. In conclusion, it is evident that temperature significantly affects crack growth.

As a note, if we add the heat transfer equation in Eq. (1), we can observe the thermal response (thermal behavior) due to crack propagation, as studied in [38]. However, we do not investigate this in the present study. Nevertheless, the reader can refer to [27] for more details.

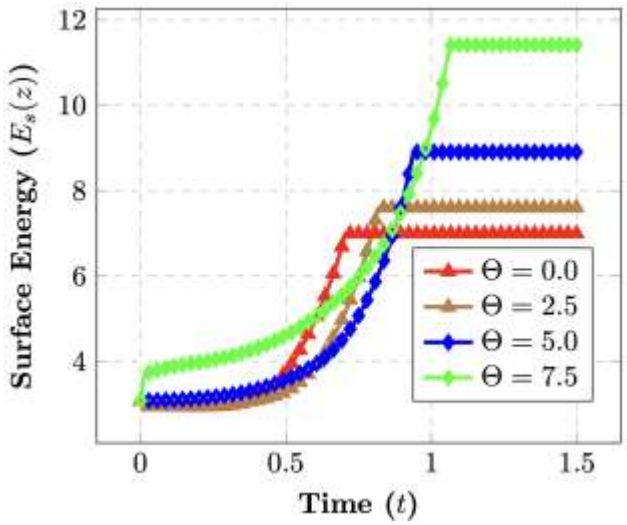

Fig. 5. Surface energy profile for each different temperature

4.2 Thermal Fracturing in a 2D Solder Domain

This section is the main focus of our research. It is divided into two parts: the first part explains solder fracturing behavior under varying maximum triangle sizes (h_{max}) while the second part addresses solder fracturing behavior due to variations in ϵ. Let us begin by studying solder fracturing behaviour under different h_{max} values.

Figure 6 shows the *z*-profile for each different maximum triangle size at times $t = 0.0, 2.5,$ and 5.0 (from left to right). As seen in Figure 6, the crack profiles are similar for each maximum triangle size. Initially, cracks appear on both sides of the solder in the right section, bordering the IC component and the PCB. These cracks then grow straight toward the left-hand side boundary. The crack tips turn approximately 45° and reach the surface of the solder at time $t = 5$. Overall, the results obtained in Figure 6 are qualitatively consistent with experimental studies [39-43] and numerical studies [8,25].

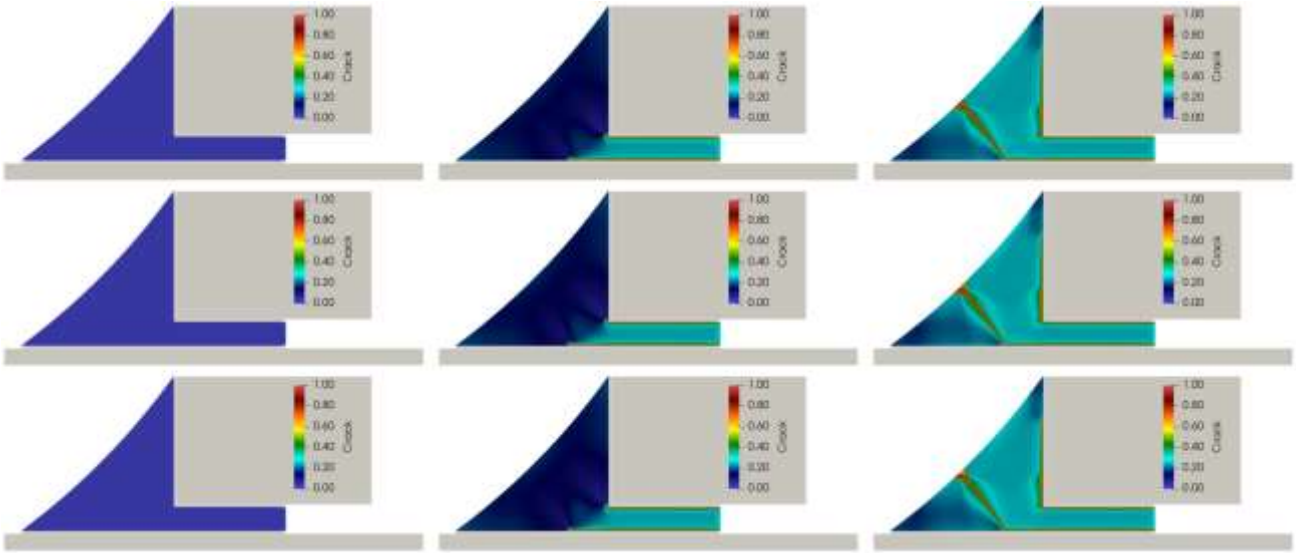

Fig. 6. Snapshot of solder fracturing for each different the maximum triangle size (h_{max}) at time $t = 0.0, 2.5, 5.0.$ (from left to right): $h_{max} = 5 \times 10^{-2}$ (top), $h_{max} = 2.5 \times 10^{-2}$ (middle), and $h_{max} = 1 \times 10^{-2}$ (bottom)

In this paper, an important point is that the numerical results of the model are supported by adaptive finite element techniques, a variant within FEM. In Figure 7, the refined mesh follows the crack path. In particular, the adaptive finite element technique positions small triangular elements around the crack, with these smaller elements highlighting stress concentrations in the solder domain. Meanwhile, larger triangular elements are used in other regions of the solder to minimize the total number of unknowns and reduce computational time. Stress concentration is determined from the displacement extrapolation of specific nodes. Therefore, this technique is highly effective for calculating and simulating crack propagation using PFM [8,26,44,45]. From this, we conclude that this technique is highly suitable for simulating crack growth.

Fig. 7. Profile of remeshing for each different $h_{max} = 0.01, 0.025, 0.05$ (from left to right) at the final time

The key advantage of applying adaptive mesh refinement is its ability to reduce computational time. As shown in Figure 8, the time consumption decreases with smaller h_{max} values. This can be explained as follows: as the number of triangles increases, the degree of freedom (DOF) also increases. The DOF is a factor that significantly influences computational time during the calculation process. This is a strong reason why we chose the adaptive mesh refinement technique.

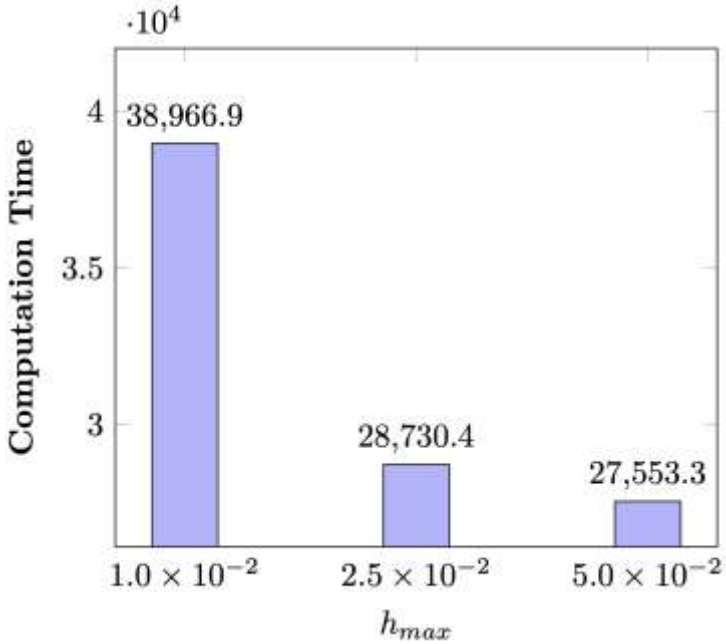

Fig. 8. Computational time for each different size of triangle h_{max}. The computation time refers to the CPU time during calculations, which is measured in seconds

Now, we address thermal fracturing behavior due to ϵ variation. Figure 9 shows the thermal fracturing in solder material due to ϵ variation. Herein, the crack profile is similar for $\epsilon = 5 \times 10^{-3}$, and $\epsilon = 7.5 \times 10^{-3}$, while it is not so similar for $\epsilon = 1 \times 10^{-3}$. Furthermore, the difference in crack

thickness is clearly visible between $\epsilon = 5 \times 10^{-3}$, $\epsilon = 7.5 \times 10^{-3}$, and $\epsilon = 1 \times 10^{-3}$. This is because the smaller the value of ϵ, the thinner the resulting crack.

As a final note, Figures 6 and 9 illustrate that the area where $z > 0$ widens as the crack length increases. This can be understood as the model implicitly assuming that the history of deformation leads to solder damage. The model is set under non-repair conditions for the crack, with $\frac{\partial z}{\partial t} \geq 0$, indicating that the recovery process of the solder material is impossible. If material deformation persists, the width of the region increases due to the assumption of damage ($\phi(x) = x_+$). Based on the findings of the present study, an interesting issue arises regarding the role of predictive maintenance in enhancing the long-term reliability of electronic devices. Regular maintenance is essential to prevent further damage to solder joints, such as crack propagation, which could ultimately lead to joint failure.

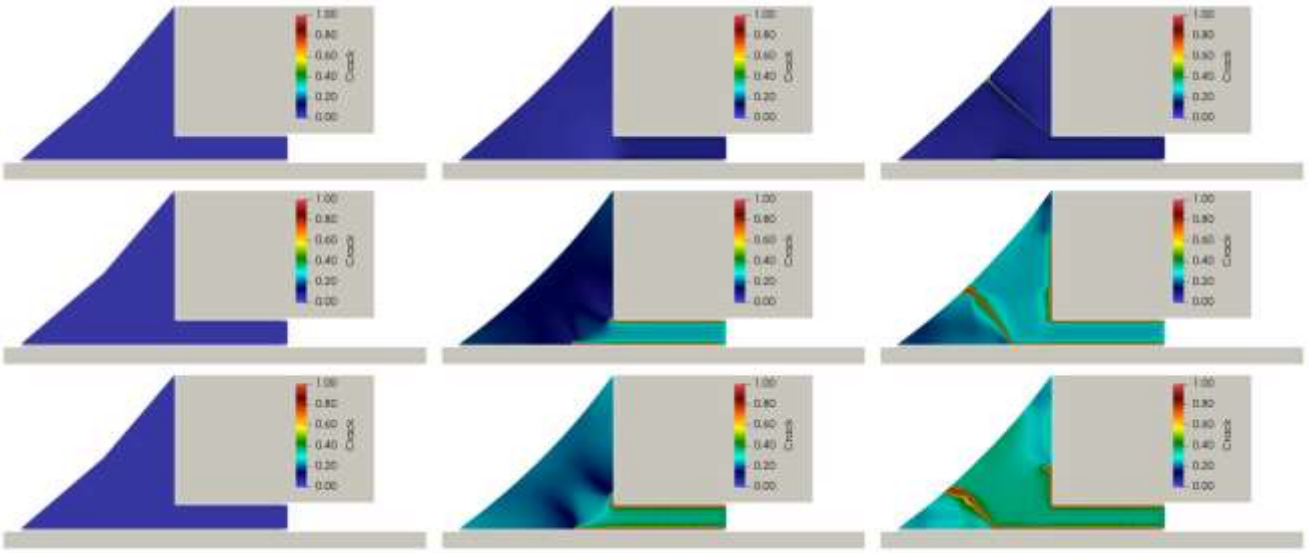

Fig. 9. Snapshot of solder fracturing for each different ϵ at time $t = 0.0, 2.5, 5.0$. (from left to right): $\epsilon = 1 \times 10^{-3}$ (top), $\epsilon = 5 \times 10^{-3}$ (middle), and $\epsilon = 7.5 \times 10^{-3}$ (bottom)

5. Summary and Future Works

A phase field model for fracturing and the finite element method (FEM) with adaptive mesh techniques have been implemented to model solder fracturing. The phase field approach is derived from the gradient flow of Francfort-Marigo type energy. In this study, because we are focusing on fracturing due to thermal effects, we include the thermal stress term in the total stress tensor. Additionally, the solder material is considered a Kelvin-Voigt type viscoelastic solid that is homogeneous and isotropic.

Although our research primarily focuses on thermal cracks in solder materials, it also examines cracks in square viscoelastic solid domains caused by temperature differences. Specifically for solder fracturing, we used a fillet-shaped solder as the domain for our model. Through numerical simulation, we demonstrated the behavior and mechanisms of solder cracking under thermal cycling stress. Overall, our results show that the findings of this study are in good agreement with previous numerical and experimental results. As a final note, the use of a small h_{max} contributes to very long computation times, while small ϵ settings result in thin crack trajectories.

To further advance this work, the Takaishi-Kimura and Alfat models, which modify the components of the stress and strain tensors, can be coupled with a general heat conduction equation [46] or a heat conduction with dua phase-lags [47] to improve results. Additionally, it is necessary to

consider the elasticity of electronic components and PCBs, as these physical objects tend to deform when subjected to a temperature field. Three-dimensional simulations will be needed to obtain a complete understanding of the cracking phenomenon in solder. Finally, an interesting area of study is the use of the Maxwell model for investigating the viscoelastic response of solder. This will be easier since we can reference several previous studies [7,48,49].

Acknowledgement
The present work was supported by DRTPM DIKTI through the Fundamental Research Scheme, grant numbers 049/E5/PG.02.00.PL/2024 and 05/UN29.20/PG/2024.

References

[1] Anam, Khairul, Anindito Purnowidodo, and Hastono Wijaya. "The Effect of Fluid Temperature and Crack Size toward Stress Intensity Factor on Geothermal Pipe Installations." Journal of Advanced Research in Fluid Mechanics and Thermal Sciences 54, no. 1 (2019): 27-36.
[2] Sokolnikoff, I. S., and E. S. Sokolnikoff. "Thermal stresses in elastic plates." Transactions of the American Mathematical Society 45, no. 2 (1939): 235-255. https://doi.org/10.1090/S0002-9947-1939-1501989-8
[3] Tanaka, Hirokazu, Yuuichi Aoki, and Shigeharu Yamamoto. "The mechanism of solder cracking." Report 2 in ESPEC Technology Report (1997): 1997.
[4] De Vries, J. W. C., M. Y. Jansen, and W. D. Van Driel. "On the difference between thermal cycling and thermal shock testing for board level reliability of soldered interconnections." Microelectronics Reliability 47, no. 2-3 (2007): 444-449. https://doi.org/10.1016/j.microrel.2006.05.009
[5] Lee, W. W., L. T. Nguyen, and Guna S. Selvaduray. "Solder joint fatigue models: review and applicability to chip scale packages." Microelectronics reliability 40, no. 2 (2000): 231-244. https://doi.org/10.1016/S0026-2714(99)00061-X
[6] Chen, S. C., Yi-Cheng Lin, and C. H. Cheng. "The numerical analysis of strain behavior at the solder joint and interface in a flip chip package." Journal of Materials Processing Technology 171, no. 1 (2006): 125-131. https://doi.org/10.1016/j.jmatprotec.2005.06.061
[7] Richardson, Casey L., Jan Hegemann, Eftychios Sifakis, Jeffrey Hellrung, and Joseph M. Teran. "An XFEM method for modeling geometrically elaborate crack propagation in brittle materials." International Journal for Numerical Methods in Engineering 88, no. 10 (2011): 1042-1065. https://doi.org/10.1002/nme.3211
[8] Kimura, Masato, Takeshi Takaishi, Sayahdin Alfat, Takumi Nakano, and Yoshimi Tanaka. "Irreversible phase field models for crack growth in industrial applications: thermal stress, viscoelasticity, hydrogen embrittlement." SN Applied Sciences 3, no. 9 (2021): 781. https://doi.org/10.1007/s42452-021-04593-6
[9] Ambati, Marreddy, Tymofiy Gerasimov, and Laura De Lorenzis. "A review on phase-field models of brittle fracture and a new fast hybrid formulation." Computational Mechanics 55 (2015): 383-405. https://doi.org/10.1007/s00466-014-1109-y
[10] Francfort, Gilles A., and J-J. Marigo. "Revisiting brittle fracture as an energy minimization problem." Journal of the Mechanics and Physics of Solids 46, no. 8 (1998): 1319-1342. https://doi.org/10.1016/S0022-5096(98)00034-9
[11] Bourdin, Blaise, Gilles A. Francfort, and Jean-Jacques Marigo. "Numerical experiments in revisited brittle fracture." Journal of the Mechanics and Physics of Solids 48, no. 4 (2000): 797-826. https://doi.org/10.1016/S0022-5096(99)00028-9
[12] Kimura, Masato, and Takeshi Takaishi. "A phase field approach to mathematical modeling of crack propagation." A Mathematical Approach to Research Problems of Science and Technology: Theoretical Basis and Developments in Mathematical Modeling (2014): 161-170. https://doi.org/10.1007/978-4-431-55060-0_13
[13] Miehe, Christian, Martina Hofacker, and Fabian Welschinger. "A phase field model for rate-independent crack propagation: Robust algorithmic implementation based on operator splits." Computer Methods in Applied Mechanics and Engineering 199, no. 45-48 (2010): 2765-2778. https://doi.org/10.1016/j.cma.2010.04.011
[14] Spatschek, Robert, Efim Brener, and Alain Karma. "Phase field modeling of crack propagation." Philosophical Magazine 91, no. 1 (2011): 75-95. https://doi.org/10.1080/14786431003773015
[15] Anderson, Daniel M., Geoffrey B. McFadden, and Adam A. Wheeler. "A phase-field model of solidification with convection." Physica D: Nonlinear Phenomena 135, no. 1-2 (2000): 175-194. https://doi.org/10.1016/S0167-2789(99)00109-8
[16] Echebarria, Blas, Roger Folch, Alain Karma, and Mathis Plapp. "Quantitative phase-field model of alloy solidification." Physical Review E—Statistical, Nonlinear, and Soft Matter Physics 70, no. 6 (2004): 061604. https://doi.org/10.1103/PhysRevE.70.061604

[17] Wang, S-L., R. F. Sekerka, A. A. Wheeler, B. T. Murray, S. R. Coriell, RJea Braun, and GB1245661 McFadden. "Thermodynamically-consistent phase-field models for solidification." Physica D: Nonlinear Phenomena 69, no. 1-2 (1993): 189-200. https://doi.org/10.1016/0167-2789(93)90189-8
[18] Kobayashi, Ryo. "Modeling and numerical simulations of dendritic crystal growth." Physica D: Nonlinear Phenomena 63, no. 3-4 (1993): 410-423. https://doi.org/10.1016/0167-2789(93)90120-P
[19] Tóth, Gyula I., György Tegze, Tamás Pusztai, Gergely Tóth, and László Gránásy. "Polymorphism, crystal nucleation and growth in the phase-field crystal model in 2D and 3D." Journal of Physics: Condensed Matter 22, no. 36 (2010): 364101. https://doi.org/10.1088/0953-8984/22/36/364101
[20] Nonomura, Makiko. "Study on multicellular systems using a phase field model." PloS one 7, no. 4 (2012): e33501. https://doi.org/10.1371/journal.pone.0033501
[21] Yang, Xiaofeng, Yi Sun, and Qi Wang. "A phase field approach for multicellular aggregate fusion in biofabrication." Journal of biomechanical engineering 135, no. 7 (2013): 071005. https://doi.org/10.1115/1.4024139
[22] Liu, Chun, and Jie Shen. "A phase field model for the mixture of two incompressible fluids and its approximation by a Fourier-spectral method." Physica D: Nonlinear Phenomena 179, no. 3-4 (2003): 211-228. https://doi.org/10.1016/S0167-2789(03)00030-7
[23] Jacqmin, David. "Calculation of two-phase Navier–Stokes flows using phase-field modeling." Journal of computational physics 155, no. 1 (1999): 96-127. https://doi.org/10.1006/jcph.1999.6332
[24] Shen, C., and Y. Wang. "Phase field model of dislocation networks." Acta materialia 51, no. 9 (2003): 2595-2610. https://doi.org/10.1016/S1359-6454(03)00058-2
[25] Sarkar, Subrato, Indra Vir Singh, and B. K. Mishra. "A Thermo-mechanical gradient enhanced damage method for fracture." Computational Mechanics 66 (2020): 1399-1426. https://doi.org/10.1007/s00466-020-01908-z
[26] Alfat, Sayahdin, Masato Kimura, and Alifian Mahardhika Maulana. "Phase field models for thermal fracturing and their variational structures." Materials 15, no. 7 (2022): 2571. https://doi.org/10.3390/ma15072571
[27] Alfat, Sayahdin. "On energy-consistency principle of PFM for thermal fracturing in thermoviscoelasticity solids and its application for modeling thermal response due to crack growth based on adaptive mesh technique." Computers & Mathematics with Applications 175 (2024): 107-118. https://doi.org/10.1016/j.camwa.2024.09.016
[28] Alfat, Sayahdin. "Phase Field Model for Crack Propagation and its Extension to Thermoelasticity and Poroelasticity: Thermal Fracturing, Hydraulic Fracturing, and Desiccation Cracking." PhD diss., Ph. D. thesis, Kanazawa University, 2023.
[29] Billotte, Catherine, Pierre J. Carreau, and Marie-Claude Heuzey. "Rheological characterization of a solder paste for surface mount applications." Rheologica Acta 45 (2006): 374-386. https://doi.org/10.1007/s00397-005-0053-3
[30] Durairaj, R., S. Ramesh, S. Mallik, A. Seman, and N. Ekere. "Rheological characterisation and printing performance of Sn/Ag/Cu solder pastes." Materials & Design 30, no. 9 (2009): 3812-3818. https://doi.org/10.1016/j.matdes.2009.01.028
[31] Mukherjee, Subhasis, Mohammed Nuhi, Abhijit Dasgupta, and Mohammad Modarres. "Creep constitutive models suitable for solder alloys in electronic assemblies." Journal of electronic packaging 138, no. 3 (2016): 030801. https://doi.org/10.1115/1.4033375
[32] Liu, Wenning, and Frank G. Shi. "Effect of the viscoelastic behavior of molding compounds on crack propagation in IC packages." In 52nd Electronic Components and Technology Conference 2002.(Cat. No. 02CH37345), pp. 854-858. IEEE, 2002. 10.1109/ECTC.2002.1008200
[33] Bui, Huy Duong, and Stéphanie Chaillat. "On a nonlinear inverse problem in viscoelasticity." Vietnam Journal of Mechanics 31, no. 3-4 (2009): 211-219. https://doi.org/10.15625/0866-7136/31/3-4/5649
[34] Lakes, Roderic S. *Viscoelastic Solids (1998)*. CRC press, 2017.
[35] Weinberg, Kerstin, Tim Dally, Stefan Schuß, Marek Werner, and Carola Bilgen. "Modeling and numerical simulation of crack growth and damage with a phase field approach." GAMM-Mitteilungen 39, no. 1 (2016): 55-77. https://doi.org/10.1002/gamm.201610004
[36] Halouani, Ayda, Abel Cherouat, Mariem Miladi Chaabane, and Mohamed Haddar. "Modeling and experimental investigation of damage initiation and propagation of LQFP package under thermal cycle." Microsystem Technologies 26 (2020): 3011-3021. https://doi.org/10.1007/s00542-020-04884-9
[37] Hecht, Frédéric. "New development in FreeFem++." Journal of numerical mathematics 20, no. 3-4 (2012): 251-266. https://doi.org/10.1515/jnum-2012-0013
[38] Ngaongam, Choosak, and Rapee Ujjin. "FEM Modelling of the Heating Behaviour in Vibrothermography Based on Thermoelastic Damping on Crack Location." Journal of Advanced Research in Fluid Mechanics and Thermal Sciences 108, no. 1 (2023): 66-74. https://doi.org/10.37934/arfmts.108.1.6674
[39] Hillman, Craig, Nathan Blattau, and Matt Lacy. "Predicting Fatigue of Solder Joints Subjected to High Number of Power Cycles." In IPC APEX EXPO Conference Proceedings. 2014.

[40] Lin, Jian, Yongping Lei, Zhongwei Wu, and LanLi Yin. "Comparison investigation of thermal fatigue and mechanical fatigue behavior of board level solder joint." In 2010 11th International Conference on Electronic Packaging Technology & High Density Packaging, pp. 1179-1182. IEEE, 2010. https://doi.org/10.1109/ICEPT.2010.5582756
[41] Lall, Pradeep, Mohd Nokibul Islam, John Evans, Jeffrey C. Suhling, and Tushar Shete. "Damage mechanics of electronics on metal-backed substrates in harsh environments." IEEE Transactions on Components and Packaging Technologies 29, no. 1 (2006): 204-212. https://doi.org/10.1109/TCAPT.2006.870390
[42] Ima, T. "Estimating the thermal fatigue life of lead-free solder joints." Yamaha Motor Tech Rev 49 (2013): 43-47.
[43] Sitek, Janusz, Aneta Araźna, Kamil Janeczek, Wojciech Stęplewski, Krzysztof Lipiec, Konrad Futera, and Piotr Ciszewski. "Influence of thermal cycling on reliability of solder joints executed on long and metal core PCBs." Soldering & Surface Mount Technology 27, no. 3 (2015): 120-124. https://doi.org/10.1108/SSMT-03-2015-0009
[44] Alfat, Sayahdin. "New Frameworks of PFM for Thermal Fracturing in The Linear Thermoelasticity Solids Based on a Microforce Balance Approach." (2023). https://doi.org/10.21203/rs.3.rs-3776383/v1
[45] Li, Yicong, Tiantang Yu, Chen Xing, and Sundararajan Natarajan. "Crack growth in homogeneous media using an adaptive isogeometric fourth-order phase-field model." Computer Methods in Applied Mechanics and Engineering 413 (2023): 116122. https://doi.org/10.1016/j.cma.2023.116122
[46] Biot, Maurice Anthony. "Thermoelasticity and irreversible thermodynamics." Journal of applied physics 27, no. 3 (1956): 240-253. https://doi.org/10.1063/1.1722351
[47] Abouelregal, Ahmed E., Fahad Alsharari, S. S. Alsaeed, Mohammed Aldandani, and Hamid M. Sedighi. "A semi-analytical approach for thermoelastic wave propagation in infinite solids subject to linear heat supply using two-phase lag theory." Continuum Mechanics and Thermodynamics (2024): 1-18. https://doi.org/10.1007/s00161-024-01324-1
[48] Shen, Rilin, Haim Waisman, and Licheng Guo. "Fracture of viscoelastic solids modeled with a modified phase field method." Computer Methods in Applied Mechanics and Engineering 346 (2019): 862-890. https://doi.org/10.1016/j.cma.2018.09.018
[49] Yin, Bo, Johannes Storm, and Michael Kaliske. "Viscoelastic phase-field fracture using the framework of representative crack elements." International Journal of Fracture 237, no. 1 (2022): 139-163. https://doi.org/10.1007/s10704-021-00522-1